Vanadium(IV) and -(V) Complexes with O,N-Chelating Aminophenolate and Pyridylalkoxide Ligands

Henk Hagen,[†] Chris Bezemer,[†] Jaap Boersma,[†] Huub Kooijman,[‡] Martin Lutz,[‡] Anthony L. Spek,[‡,§] and Gerard van Koten*[,†]

Debye Institute, Department of Metal-Mediated Synthesis, Utrecht University, Padualaan 8, 3584 CH Utrecht, The Netherlands, and Bijvoet Center for Biomolecular Research, Crystal and Structural Chemistry, Utrecht University, Padualaan 8, 3584 CH Utrecht, The Netherlands

Received December 8, 1999

Two different monoanionic O,N-chelating ligand systems, i.e., $[OC_6H_2(CH_2NMe_2)$-2-Me_2-4,6$]^-$ (**1**) and $[OCMe_2$([2]-Py)$]^-$ (**2**), have been applied in the synthesis of vanadium(V) complexes. The tertiary amine functionality in **1** caused reduction of the vanadium nucleus to the 4+ oxidation state with either $[VOCl_3]$, $[V(=NR)Cl_3]$, or $[V(=NR)(NEt_2)_3]$ (R = Ph, (**3a**, **5a**), R = *p*-Tol (**3b**, **5b**)), and applying **1** as a reducing agent resulted in the synthesis of the vanadium(IV) complexes $[VO(OC_6H_2(CH_2NMe_2)$-2-Me_2-4,6$)_2]$ (**4**) and $[V(=NPh)(OC_6H_2(CH_2$-$NMe_2)$-2-Me_2-4,6$)_2]$ (**6**). In the case of $[V(=N$-*p*-Tol$)(NEt_2)(OC_6H_2(CH_2NMe_2)$-2-$Me_2$-4,6$)_2]$ (**7b**), the reduction was sufficiently slow to allow its characterization by ^{1}H NMR and variable-temperature studies showed it to be a five-coordinate species in solution. Although the reaction of **1** with $[V(=N$-*p*-Tol$)(O$-*i*-Pr$)_3]$ (**9b**) did not result in reduction of the vanadium nucleus, vanadium(V) compounds could not be isolated. Mixtures of the vanadium(V) (mono)phenolate, $[V(=N$-*p*-Tol$)(O$-*i*-Pr$)_2(OC_6H_2(CH_2NMe_2)$-2-Me_2-4,6$)]$ (**10**), and the vanadium(V) (bis)phenolate, $[V(=N$-*p*-Tol$)(O$-*i*-Pr$)(OC_6H_2(CH_2NMe_2)$-2-Me_2-4,6$)_2]$ (**11**), were obtained. With the pyridylalkoxide **2,** no reduction was observed and the vanadium(V) compounds $[VOCl_2(OCMe_2$([2]-Py$))]$ (**12**) and $[V(=N$-*p*-Tol$)Cl_2(OCMe_2$([2]-Py$)]$ (**13**) were obtained. ^{51}V NMR showed **7b** and **12** to be five-coordinate in solution, whereas for **10**, **11**, and **13** a coordination number of 6 was found. Compounds **12** and **13** showed decreased activity compared to their nonchelated vanadium(V) analogues when applied as catalysts in ethene polymerization. Two polymorphic forms with a difference in the V−N−C angle of 12.5° have been found for **6**. Crystal data: **6**·Et_2O, triclinic, $P\bar{1}$, a = 11.1557(6) Å, b = 12.5744(12) Å, c = 13.1051(14) Å, α = 64.244(8)°, β = 70.472(7)°, γ = 87.950(6)°, V = 1547(3) Å^3, Z = 2; **6**·C_6H_6, triclinic, $P\bar{1}$, a = 8.6034(3) Å, b = 13.3614(4) Å, c = 15.1044(5) Å, α = 98.182(3)°, β = 105.618(2)°, γ = 107.130(2)°, V = 1551.00(10) Å^3, Z = 2; **12**, orthorhombic, *Pbca*, a = 11.8576(12) Å, b = 12.6710(13) Å, c = 14.722(2) Å, V = 2211.9(4) Å^3, Z = 8.

Introduction

Recently we set out to study the use of monoanionic potentially bidentate phenolate or alkoxide ligands, i.e., $[OC_6H_2(CH_2NMe_2)$-2-Me_2-4,6$]^-$ (O-MDMBA) (**1**) and α,α-dimethyl-2-pyridyl methoxide $[OCMe_2$([2]-Py$)]^-$ (**2**) (see Figure 1), in vanadium(V) chemistry. These ligands have been chosen since vanadium catalyst systems with oxygen-containing ligands are known to give polymers with narrow molecular weight distributions,[1] while the nitrogen donor atom in the ligands can help in stabilizing the high oxidation state of the vanadium center by V−N coordination. In addition to the latter effect, an *o*-amino functionality itself represents a substituent with considerable bulk, which can prevent bimolecular deactivation pathways of the vanadium(V) catalyst.[2−4] Finally, the electronic properties of the vanadium center can be influenced considerably by varying the substituents on the ring, as we have recently shown for vanadium(IV) oxo (bis)phenolate complexes.[5]

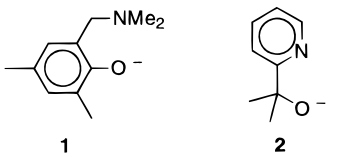

1 2

Figure 1. Selected potentially O,N-chelating monoanionic ligands. Abbreviations used: **1**, [O-MDMBA]$^-$; **2**, $[OCMe_2$([2]-Py$)]^-$.

Another way of stabilizing a high oxidation state vanadium center is the use of imido ligands. These are more electron-donating than an oxo group due to their reduced electronegativity.[6] Moreover, the vanadium center can be influenced both electronically and sterically, when an organic group is present on the imido nitrogen. For these studies we have used both the

* To whom correspondence should be addressed. E-mail: g.vankoten@chem.uu.nl.

† Debye Institute, Department of Metal-Mediated Synthesis.

‡ Bijvoet Center for Biomolecular Research, Crystal and Structural Chemistry.

§ To whom correspondence pertaining to crystallographic studies should be addressed. E-mail: a.l.spek@chem.uu.nl.

(1) Karol, F. J.; Kao, S.-C. *New J. Chem.* **1994**, *18*, 97.
(2) Murphy, V. J.; Turner, H. *Organometallics* **1997**, *16*, 2495 and references therein.
(3) Preuss, F.; Becker, H.; Kaub, J.; Sheldrick, W. S. *Z. Naturforsch.* **1988**, *43b*, 1195.
(4) Buijink, J.-K. F.; Meetsma, A.; Teuben, J. H.; Kooijman, H.; Spek, A. L. *J. Organomet. Chem.* **1995**, *497*, 161.
(5) Hagen, H.; Barbon, A.; van Faassen, E. E.; Lutz, B. T. G.; Boersma, J.; Spek, A. L.; van Koten, G. *Inorg. Chem.* **1999**, *38*, 4079.
(6) Nugent, W. A.; Mayer, J. M. *Metal-ligand Multiple Bonds*; John Wiley & Sons: New York, 1988.
(7) Devore, D. D.; Lichtenhan, J. D.; Takusagawa, F.; Maatta, E. A. *J. Am. Chem. Soc.* **1987**, *109*, 7408.

10.1021/ic991415s CCC: $19.00
Published on Web 08/11/2000

phenyl- and the *p*-tolylimido ligands. The latter is slightly more electron-donating[7] and has the advantage that the *p*-methyl group and the aromatic protons give very distinctive signals in the ^{1}H NMR.

In order to synthesize vanadium(V) complexes with the O,N-chelating ligands, we have used three types of starting material, viz., vanadium(V) chlorides, diethylamides, and isopropoxides. The O,N-chelating vanadium(V) products as well as several vanadium(V) starting materials were tested in ethene polymerization with Et_2AlCl as cocatalyst.

Experimental Section

General. All reactions were performed in an atmosphere of dry, oxygen-free dinitrogen using standard Schlenk techniques. Solvents were carefully dried and distilled prior to use. $HOC_6H_2(CH_2NMe_2)$-2-Me_2-4,6 (**1**),[8] [V(═NPh)Cl_3] (**3a**) and [V(═N-*p*-tol)Cl_3] (**3b**),[7] [V(═N-*p*-Tol)(O-*i*-Pr)$_3$] (**9b**),[9] [VO(O-*i*-Pr)$_3$] (**8**),[10] and $LiOCMe_2$([2]-Py)[11] were prepared according to literature procedures. Et_3N was distilled from CaH_2. All other chemicals were obtained from commercial sources and used as received. Elemental analyses were performed by H. Kolbe, Mikroanalytisches Laboratorium, Mülheim, Germany. ^{1}H and ^{13}C NMR spectra were recorded on a Bruker AC200 or 300 spectrometer or a Varian Inova 300 spectrometer. ^{51}V NMR spectra were recorded on a Bruker AC300 spectrometer at 78.9 MHz relative to an external standard ([$VOCl_3$]/$CDCl_3$, 75/25 v/v).[12] EPR spectra were recorded on a Bruker ESP 300 spectrometer.

Synthesis of [VO(OC$_6$H$_2$(CH$_2$NMe$_2$)-2-Me$_2$-4,6)$_2$] (4). A mixture of $HOC_6H_2(CH_2NMe_2)$-2-Me_2-4,6 (**1**) (1.90 g, 10.6 mmol) and Et_3N (2 mL, excess) in C_6H_6 (50 mL) was added to a stirred solution of [$VOCl_3$] (0.74 g, 4.2 mmol) in C_6H_6 (10 mL) in 15 min. After stirring for 16 h the solvent was removed in vacuo. The residue was washed with nitrogen-flushed MeOH (2 × 150 mL) to give [VO($OC_6H_2(CH_2NMe_2)$-2-Me_2-4,6)$_2$] as a purple solid (1.41 g; 80%). Crystallization from $MeNO_2$ at room temperature gave blue crystals. Mp: 205 °C.

Anal. Calcd for $C_{22}H_{32}N_2O_3V$: C, 62.40; H, 7.62; N, 6.62. Found: C, 62.26; H, 7.58; N, 6.56.

Synthesis of [V(═NPh)(NEt$_2$)$_3$] (5a). A solution of $LiNEt_2$ (1.43 g, 18.1 mmol) in Et_2O (75 mL) was added dropwise to a stirred solution of [V(═NPh)Cl_3] (**3a**) (1.46 g, 5.9 mmol) in Et_2O (75 mL) at 0 °C. After stirring for 16 h at room temperature the white precipitate was removed from the solution by centrifugation/decantation. The supernatant solution was evaporated to dryness in vacuo, and the residue was extracted with hexane (150 mL). Removal of the hexane in vacuo afforded [V(═NPh)(NEt$_2$)$_3$] as a red oil (2.11 g, 100%).

^{1}H NMR (300 MHz, C_6D_6): δ 1.16 (t, 18 H, $^3J_{H,H}$ = 7.0 Hz, N(CH_2CH_3)$_2$), 3.77 (q, 12 H, $^3J_{H,H}$ = 7.0 Hz, N(CH_2CH_3)$_2$) 6.80−7.30 (m, 5 H, NPh−H).

^{51}V NMR (78.9 MHz, C_6D_6): δ −172 (partially resolved triplet, $^1J_{^{51}V,^{14}N}$ = 97 Hz, $\Delta\nu_{1/2}$ = 276 Hz).

Synthesis of [V(═N-*p*-Tol)(NEt$_2$)$_3$] (5b). $LiNEt_2$ (2.04 g, 25.8 mmol) in Et_2O (40 mL) was added to a stirred suspension of [V(═N-*p*-Tol)Cl_3] (**3b**) (2.07 g, 7.9 mmol) in Et_2O (30 mL) at 0 °C. After stirring for 3 h at room temperature the solvent was removed in vacuo. The remaining solid was extracted with pentane (50 mL). Removal of the volatiles in vacuo yielded a red oil (2.74 g, 92%).

^{1}H NMR (300 MHz, C_6D_6): δ 1.18 (t, 18 H, $^3J_{H,H}$ = 7.0 Hz, N(CH_2CH_3)$_2$), 2.11 (s, 3 H, NAr−*Me*), 3.78 (q, 12 H, $^3J_{H,H}$ = 7.0 Hz, N(CH_2CH_3)$_2$), 6.92 and 7.21 (AB, 4 H, $^3J_{H,H}$ = 8.0 Hz, N−Ar).

^{51}V NMR (78.9 MHz, C_6D_6): δ −175 (partially resolved triplet, $^1J_{^{51}V,^{14}N}$ = 99 Hz, $\Delta\nu_{1/2}$ = 275 Hz).

Synthesis of [V(═NPh)(OC$_6$H$_2$(CH$_2$NMe$_2$)-2-Me$_2$-4,6)$_2$] (6). To a stirred solution of [V(═NPh)(NEt$_2$)$_3$] (**5a**) (1.54 g, 4.3 mmol) in Et_2O (50 mL) was added a solution of $HOC_6H_2(CH_2NMe_2)$-2-Me_2-4,6 (**1**) (0.78 g, 4.4 mmol) in Et_2O (10 mL) at 0 °C. The resulting mixture was stirred for 2 days, after which it was filtered. Cooling the filtrate to −20 °C gave dark-red crystals (0.86 g, 35%). Mp: 178 °C.

Anal. Calcd for $C_{28}H_{37}N_3O_2V\cdot Et_2O$: C, 67.11; H, 8.27; N, 7.34. Found: C, 66.96; H, 8.25; N, 7.37.

EPR (hexane, 7.3 mM): A_{iso} = 85.28 × 10^{-4} cm^{-1}, g_{iso} = 1.9717.

Synthesis of [V(═NPh)(NEt$_2$)(OC$_6$H$_2$(CH$_2$NMe$_2$)-2-Me$_2$-4,6)$_2$] (7a). $HOC_6H_2(CH_2NMe_2)$-2-Me_2-4,6 (**1**) (0.90 g, 5.0 mmol) was added slowly to [V(═NPh)(NEt$_2$)$_3$] (**5a**) (0.90 g, 2.5 mmol) in hexane (50 mL) at 0 °C. After stirring for 2 h at room temperature the solvent was removed in vacuo, leaving a brown-red solid in quantitative yield.

^{1}H NMR (200 MHz, C_6D_6): δ 0.88 (bs, 6 H, N(CH_2CH_3)$_2$), 2.29 (s, 6 H, *p*-Me), 2.36 (s, 12 H, NMe_2), 2.50 (s, 6 H, *o*-Me), 3.41 and 4.07 (AB, 4 H, $^2J_{H,H}$ = 13.5 Hz, CH_2NMe_2), 4.48 (bs, 4 H, N(CH_2CH_3)$_2$), 6.68−7.24 (m, 9 H, Ar−H).

Synthesis of [V(═N-*p*-Tol)(NEt$_2$)(OC$_6$H$_2$(CH$_2$NMe$_2$)-2-Me$_2$-4,6)$_2$] (7b). $HOC_6H_2(CH_2NMe_2)$-2-Me_2-4,6 (**1**) (1.70 g, 9.5 mmol) in pentane (20 mL) was added to [V(═N-*p*-Tol)(NEt$_2$)$_3$] (**5b**) (1.77 g, 4.7 mmol) in pentane (40 mL) over a period of 30 min. After stirring for 2 h at room temperature residual solid material was removed by centrifugation/decantation. Subsequent removal of the solvent in vacuo gave an orange-red solid in quantitative yield.

^{1}H NMR (300 MHz, C_6D_6): δ 0.80 (bs, 6 H, N(CH_2CH_3)$_2$), 2.01 (s, 3 H, NAr−*Me*), 2.29 (s, 6 H, *p*-Me), 2.38 (s, 12 H, NMe_2), 2.50 (s, 6 H, *o*-Me), 3.44 and 4.11 (AB, 4 H, $^2J_{H,H}$ = 13.5 Hz, CH_2NMe_2), 4.50 (bs, 4 H, N(CH_2CH_3)$_2$), 6.74 and 7.17 (AB, 4 H, $^3J_{H,H}$ = 8.2 Hz, N−Ar), 6.97 (s, 2 H, *m*-H), 6.99 (s, 2 H, *m*-H).

^{51}V NMR (78.9 MHz, C_6D_6): δ −235 ($\Delta\nu_{1/2}$ = 137 Hz).

Synthesis of [V(═NPh)(O-*i*-Pr)$_3$] (9a). Phenyl isocyanate (2.11 mL, 19.4 mmol) was added to a stirred solution of [VO(O-*i*-Pr)$_3$] (**8**) (4.73 g, 19.4 mmol) in octane (30 mL). After refluxing for 3 h the solvent was removed in vacuo. Recrystallization from hexane at −30 °C yielded orange-brown crystals (4.09 g, 66%). Mp: 53 °C.

Anal. Calcd for $C_{15}H_{26}NO_3V$: C, 56.42; H, 8.21; N, 4.39. Found: C, 56.58; H, 8.11; N, 4.36.

^{1}H NMR (200 MHz, $CDCl_3$): δ 1.38 (d, 18 H, $^3J_{H,H}$ = 6.1 Hz, OCH*Me*$_2$), 5.15 (sept, 3 H, $^3J_{H,H}$ = 6.1 Hz, OC*H*Me_2), 7.05−7.29 (bm, 5 H, NAr).

^{13}C NMR (50 MHz, $CDCl_3$): δ 26.9 (OCH*Me*$_2$), 80.2 (broad, OC*H*Me_2), 125.2 (NAr−C^2 and NAr−C^6), 125.5 (NAr−C^3 and NAr−C^5) 128.5 (NAr−C^4), NAr−C^1 not observed.

^{51}V NMR (78.9 MHz, $CDCl_3$) δ −622 ($t_{1:1:1}$, $^1J_{^{51}V,^{14}N}$ = 113 Hz).

Attempted Synthesis of [V(═N-*p*-Tol)(O-*i*-Pr)$_2$(OC$_6$H$_2$(CH$_2$NMe$_2$)-2-Me$_2$-4,6)] (10). To a solution of [V(═N-*p*-Tol)(O-*i*-Pr)$_3$] (**9b**) (0.55 g, 1.7 mmol) in pentane (25 mL) was added $HOC_6H_2(CH_2NMe_2)$-2-Me_2-4,6 (**1**) (0.30 g, 1.7 mmol) in pentane (10 mL). After stirring for 24 h the solvent was removed in vacuo, leaving a dark-red oil. ^{1}H NMR analysis showed the oil to be a mixture of [V(═N-*p*-Tol)(O-*i*-Pr)$_3$] (**9b**), the monophenolate [V(═N-*p*-Tol)(O-*i*-Pr)$_2$($OC_6H_2(CH_2NMe_2)$-2-Me_2-4,6)] (**10**), and the (bis)phenolate [V(═N-*p*-Tol)(O-*i*-Pr)($OC_6H_2(CH_2NMe_2)$-2-Me_2-4,6)$_2$] (**11**) in a 1:2:1 ratio.

^{1}H NMR (300 MHz, C_6D_6): for **10**, δ 1.26 (d, 6 H, $^3J_{H,H}$ = 6 Hz, OCH*Me*$_2$), 1.40 (d, 6 H, $^3J_{H,H}$ = 6 Hz, OCH*Me*$_2$), 2.05 (s, 3 H, NAr−*Me*), 2.14 (s, 3 H, OAr−*Me*), 2.22 (s, 3 H, OAr−*Me*), 2.34 (s, 6 H, NMe_2), 3.71 (s, 2 H, CH_2), 5.90 (sept, 2 H, $^3J_{H,H}$ = 6 Hz, OC*H*Me_2), 6.83 and 7.44 (AB, 4 H, $^3J_{H,H}$ = 8 Hz, N−Ar); for **11**, δ 1.34 (d, 6 H, $^3J_{H,H}$ = 6 Hz, OCH*Me*$_2$), 1.89 (s, 3 H, NAr−*Me*), 2.24 (s, 6 H, OAr−*Me*), 2.27 (s, 12 H, NMe_2), 2.47 (s, 6 H, OAr−*Me*), 3.57 and 3.88 (AB, 4 H, $^2J_{H,H}$ = 13 Hz, CH_2), 5.96 (sept, 1 H, $^3J_{H,H}$ = 6 Hz, OC*H*Me_2), 6.59 and 6.71 (AB, 4 H, $^3J_{H,H}$ = 8 Hz, N−Ar).

^{51}V NMR (78.9 MHz, $CDCl_3$): for **10**, δ −444 ($\Delta\nu_{1/2}$ = 450 Hz); for **11**, δ −358 ($\Delta\nu_{1/2}$ = 808 Hz).

Attempted Synthesis of [V(═N-*p*-Tol)(O-*i*-Pr)(OC$_6$H$_2$(CH$_2$NMe$_2$)-2-Me$_2$-4,6)$_2$] (11). To a solution of [V(═N-*p*-Tol)(O-*i*-Pr)$_3$] (**9b**) (0.88 g, 2.6 mmol) in Et_2O (25 mL) was added $HOC_6H_2(CH_2NMe_2)$-2-Me_2-4,6 (**1**) (0.96 g, 5.4 mmol) in Et_2O (10 mL). After stirring for 16 h the

(8) van der Schaaf, P. A.; Jastrzebski, J. T. B. H.; Hogerheide, M. P.; Smeets, W. J. J.; Spek, A. L.; van Koten, G. *Inorg. Chem.* **1993**, *32*, 4111.
(9) Lutz, M.; Hagen, H.; Schreurs, A. M. M.; Spek, A. L.; van Koten, G. *Acta Crystallogr.* **1999**, *C55*, 1636.
(10) Prandtl, W.; Hess, L. *Z. Anorg. Chem.* **1913**, *82*, 103.
(11) van der Schaaf, P. A.; Boersma, J.; Smeets, W. J. J.; Spek, A. L.; van Koten, G. *Inorg. Chem.* **1993**, *32*, 5108.
(12) Rehder, D. In *Studies in Inorganic Chemistry 13: Transition Metal NMR*; Pregosin, P. S., Ed.; Elsevier: Amsterdam, The Netherlands, 1991.

Table 1. Crystallographic Data for **6**·Et_2O, **6**·C_6H_6, and **12**

	6·Et_2O	**6**·C_6H_6	**12**
empirical formula	$C_{28}H_{37}N_3O_2V$·Et_2O[a]	$C_{28}H_{37}N_3O_2V$·C_6H_6	$C_8H_{10}Cl_2NO_2V$
fw	572.69[a]	576.65	274.01
cryst syst	triclinic	triclinic	orthorhombic
space group	$P\bar{1}$ (No. 2)	$P\bar{1}$ (No. 2)	*Pbca* (No. 61)
a, Å	11.1557(6)	8.6034(3)	11.8576(12)
b, Å	12.5744(12)	13.3614(4)	12.6710(13)
c, Å	13.1051(14)	15.1044(5)	14.722(2)
α, deg	64.244(8)	98.182(3)	90
β, deg	70.472(7)	105.618(2)	90
γ, deg	87.950(6)	107.130(2)	90
V, Å^3	1547.4(3)	1551.0(1)	2211.9(4)
Z	2	2	8
D_{calcd}, g cm^{-3} [a]	1.229	1.235	1.646
μ(Mo Kα), mm^{-1}	0.4	0.4	1.4
F(000)[a]	614	614	1104
T, K	150	150	225
final R1[b]	0.0666	0.0575	0.0520
final wR2[c]	0.1634	0.1590	0.1378
goodness of fit	0.96	1.06	1.04

[a] With disordered solvent contribution. [b] $R1 = \Sigma||F_o| - |F_c||/\Sigma|F_o|$. [c] $wR2 = [\Sigma[w(F_o^2 - F_c^2)^2]/\Sigma[w(F_o^2)^2]]^{1/2}$.

solvent was removed in vacuo, leaving a dark-red oil. This oil was extracted with pentane (50 mL). Removal of the solvent in vacuo gave a dark-red sticky solid (1.53 g). ^{1}H NMR analysis showed the product to be a mixture of $HOC_6H_2(CH_2NMe_2)$-2-Me_2-4,6 (**1**), the monophenolate [V(=N-*p*-Tol)(O-*i*-Pr)$_2$($OC_6H_2(CH_2NMe_2)$-2-Me_2-4,6)] (**10**), and the (bis)phenolate [V(=N-*p*-Tol)(O-*i*-Pr)($OC_6H_2(CH_2NMe_2)$-2-Me_2-4,6)$_2$] (**11**) in a 1:1:2 ratio.

Synthesis of [$VOCl_2$($OCMe_2$([2]-Py))] (12). A suspension of $LiOCMe_2$([2]-Py) (1.43 g, 8.6 mmol) in toluene (50 mL) was added to a stirred solution of [$VOCl_3$] (1.51 g, 8.7 mmol) in pentane (40 mL). The solution turned dark-red immediately, and an orange solid precipitated. The mixture was stirred for 16 h. The resulting pale-orange solution was separated from the precipitate by centrifugation/decantation. The residue was extracted with CH_2Cl_2 (2 × 40 mL), and the volume of the combined fractions was reduced to 40 mL in vacuo. Addition of an equal amount of Et_2O followed by reduction of the volume to 15 mL in vacuo resulted in the precipitation of a yellow-orange solid. Decantation of the supernatant solution followed by washing with Et_2O (25 mL) and drying in vacuo gave [$VOCl_2$($OCMe_2$([2]-Py))] (0.90 g, 38%). Combining the supernatant solution with the ethereal fraction and leaving this solution to stand for 2 days at room temperature gave a second crop (0.47 g; 20%). Mp: 150 °C.

Anal. Calcd for $C_8H_{10}NO_2VCl_2$: C, 35.07; H, 3.68; N, 5.11. Found: C, 35.02; H, 3.72; N, 5.11.

^{1}H NMR (300 MHz, $CDCl_3$): δ 1.98 (s, 6 H, $OCMe_2$), 7.39 (d, 1 H, $^3J_{H,H}$ = 7.7 Hz, Py−H), 7.48 (t, 1 H, $^3J_{H,H}$ = 6.5 Hz, Py−H), 8.05 (t, 1 H, $^3J_{H,H}$ = 7.3 Hz, Py−H), 8.74 (d, 1 H, $^3J_{H,H}$ = 5.4 Hz, Py−H).

^{51}V NMR (78.9 MHz, $CDCl_3$): δ −235 ($\Delta\nu_{1/2}$ = 93 Hz).

Synthesis of [V(=N-*p*-Tol)Cl_2($OCMe_2$([2]-Py))] (13). $LiOCMe_2$([2]-Py) (1.10 g, 6.6 mmol) was added as a solid to a stirred solution of [V(=N-*p*-Tol)Cl_3] (**3b**) (1.72 g, 6.6 mmol) in C_6H_6 (100 mL), and the mixture was stirred for 3 h. The greenish solution was separated from the precipitate by centrifugation. The remaining solid was extracted with C_6H_6 (50 mL). The volume of the combined fractions was reduced to 50 mL in vacuo. Pentane (100 mL) was added, and the solution was left to stand for 2 weeks, affording dark greenish-blue crystalline material (1.40 g, 58%). Recrystallization from $CHCl_3$ gave dark-green needle-shaped crystals, which turned red-brownish upon drying. Mp: >200 °C.

Anal. Calcd for $C_{15}H_{17}N_2OVCl_2$·0.4$CHCl_3$: C, 45.01; H, 4.27; N, 6.82. Found: C, 45.65; H, 4.04; N, 6.81.

^{1}H NMR (300 MHz, $CDCl_3$): δ 1.77 (s, 6 H, $OCMe_2$), 2.41 (s, 3 H, NAr−*Me*), 7.05 and 7.26 (AB, 4 H, $^3J_{H,H}$ = 8.4 Hz, N−Ar), 7.4 (m, 2 H, Py−H^3 and Py−H^5), 7.94 (double t, 1 H, $^3J_{H,H}$ = 7.7 Hz, $^4J_{H,H}$ = 1.1 Hz, Py−H^4), 8.84 (d, 1 H, $^3J_{H,H}$ = 5.4 Hz, Py−H^6).

^{13}C NMR (75.5 MHz, $CDCl_3$): δ 21.6 (NAr−*Me*), 30.6 ($OCMe_2$), 96.7 ($OCMe_2$), 120.2, 123.8 (Py−C^3 and Py−C^5), 126.7 (NAr−C^2 and NAr−C^6), 128.7 (NAr−C^3 and NAr−C^5), 139.9 (Py−C^4), 140.4 (NAr−C^4), 148.7 (Py−C^6), 162.6 (NAr−C^1), 170.2 (Py−C^2).

^{51}V NMR (78.9 MHz, $CDCl_3$): δ 33 ($\Delta\nu_{1/2}$ = 1100 Hz).

Synthesis of [$VOCl_2$(O-*i*-Pr)] (14). To a solution of [VO(O-*i*-Pr)$_3$] (**8**) (1.75 g, 7.2 mmol) in toluene (25 mL) was added dropwise [$VOCl_3$] (1.35 mL, 14.3 mmol). The color changed from colorless to dark-red. The solvent was removed in vacuo, and the residue was stripped once with pentane (25 mL), leaving a dark-red liquid. Flash distillation gave a dark-orange liquid (3.61 g, 85%). Due to the volatile nature of this compound a membrane pump (working pressure approximately 10 mbar) was used instead of an oil pump.

^{1}H NMR (300 MHz, $CDCl_3$): δ 1.68 (d, 6 H, $^3J_{H,H}$ = 6.2 Hz, OCHMe_2), 6.96 (br, 1 H, OC*H*Me_2).

X-ray Crystallographic Structure Determination and Refinements. Dark-red crystals of **6** suitable for X-ray diffraction were grown either from Et_2O at −20 °C or from benzene at room temperature. Bright-orange crystals of **12** were grown from a 1:1 mixture of CH_2Cl_2 and Et_2O at −20 °C. Crystals suitable for X-ray structure determination were glued to the top of a Lindemann-glass capillary and transferred into a cold nitrogen stream on an Enraf-Nonius CAD4-T diffractometer (**6**·Et_2O, **12**) or on a Nonius KappaCCD diffractometer (**6**·C_6H_6, **9b**), both on rotating anodes. Crystal data and details on data collection are collected in Table 1. Data were collected using graphite-monochromated Mo Kα radiation (λ = 0.71073 Å). Data were corrected for *Lp* effects but not for absorption. The structure of **6**·C_6H_6 was solved by automated direct methods (SIR-97[13]).The other structures were solved by automated Patterson methods and subsequent difference Fourier techniques (SHELXS-86[14] for **6**·Et_2O, DIRDIF-92[15] for **12**). Refinement on F^2 was carried out using full-matrix least-squares techniques (SHELXL-97[16]); no observance criterion was applied during refinement. For all compounds refinement converged with $\Delta/\sigma_{max} < 0.01$ and $\Delta/\sigma_{av} < 0.01$. Hydrogen atoms were included in the refinement. All non-hydrogen atoms were refined with anisotropic displacement parameters. The hydrogen atoms were included in the refinement with a fixed isotropic atomic displacement parameter related to the value of the equivalent isotropic atomic displacement parameter of their carrier atoms.

(13) Altomare, A.; Burla, M. C.; Camalli, M.; Cascarano, G. L.; Giacovazzo, C.; Guagliardi, A.; Moliterni, A. G. G.; Polidori, G.; Spagna, R. *J. Appl. Crystallogr.* **1999**, *32*, 115.

(14) Sheldrick, G. M. *SHELXS-86 Program for crystal structure determination*; University of Göttingen: Göttingen, Germany, 1986.

(15) Beurskens, P. T.; Admiraal, G.; Beurskens, G.; Bosman, W. P.; García-Granda, S.; Gould, R. O.; Smits, J. M. M.; Smykalla, C. *The DIRDIF program system, Technical report of the Crystallography Laboratory*; University of Nijmegen: Nijmegen, The Netherlands, 1992.

(16) Sheldrick, G. M. *SHELXL-97 Program for crystal structure refinement*; University of Göttingen: Göttingen, Germany, 1997.

Scheme 1

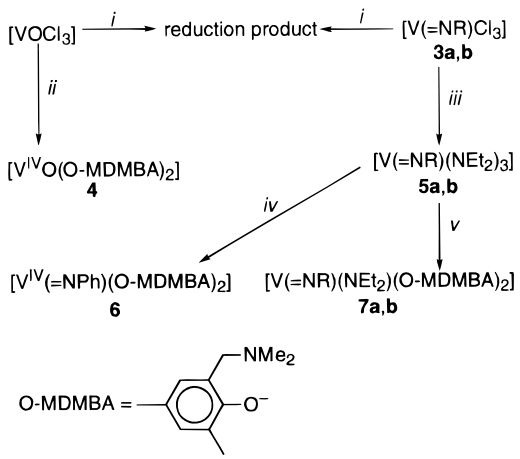

(i) 1 equiv of RO-MDMBA (R = H, $SiMe_3$, Li, Na). (ii) 2.5 equiv of HO-MDMBA, excess Et_3N, C_6H_6, room temperature. (iii) R = Ph (**a**), *p*-Tol (**b**); 3.3 equiv of $LiNEt_2$, Et_2O, 0 °C. (iv) R = Ph; 1 equiv of HO-MDMBA, hexane, 0 °C. (v) R = Ph (**a**), *p*-Tol (**b**); 2 equiv of HO-MDMBA, hexane, room temperature.

For **6**·Et_2O 7723 reflections were measured ($1.8° < \theta < 27.5°$, $-14 < h < 8$, $-16 < k < 16$, $-17 < l < 16$), 7094 of which were unique ($R_{int} = 0.0745$) using a dark-red crystal of approximate dimensions $0.1 \times 0.4 \times 0.4$ mm; 315 parameters were refined, and the final residual density was in the range $-0.37 < \Delta\rho < 0.42$ e/Å^3. The structure contained Et_2O as disordered solvent. The associated contribution to the structure factors was taken into account using the SQUEEZE procedure as incorporated in PLATON.[17] Eighty-one electrons were found in a solvent area of 320 Å^3, consistent with one solvent molecule per vanadium complex.

For **6**·C_6H_6 18775 reflections were measured ($1.6° < \theta < 25.0°$, $-10 < h < 10$, $-15 < k < 15$, $-17 < l < 17$), 5418 of which were unique ($R_{int} = 0.0530$) using a brown crystal of approximate dimensions $0.03 \times 0.21 \times 0.27$ mm; 361 parameters were refined, and the final residual density was in the range $-0.51 < \Delta\rho < 0.54$ e/Å^3.

For **12** 2992 reflections were measured ($2.7° < \theta < 27.5°$, $-15 < h < 0$, $-16 < k < 0$, $-19 < l < 12$), 2533 of which were unique ($R_{int} = 0.071$) using a bright-orange crystal of approximate dimensions $0.1 \times 0.5 \times 0.6$ mm; 129 parameters were refined, and the final residual density was in the range $-0.54 < \Delta\rho < 0.39$ e/Å^3.

Neutral atom scattering factors and anomalous dispersion corrections were taken from the *International Tables for Crystallography*.[18] Geometrical calculations and illustrations were performed with PLATON.[17]

Results and Discussion

Initial attempts to prepare vanadium(V) complexes with the *o*-aminophenolate anion **1** were carried out by adding the parent phenol, the lithium phenolate or sodium phenolate, or the corresponding trimethylsilyl ether to vanadium arylimido trichloride, [V(=NR)Cl_3] (R = Ph (**3a**), *p*-Tol (**3b**)) (Scheme 1, i). These reactions were generally accompanied by a color change from red/orange to very dark blue or green. On the basis of both the lack of signal in the ^{1}H NMR and the presence of a strong eight-line signal in the EPR, it was concluded that the vanadium was no longer in the formal 5+ oxidation state and that a paramagnetic vanadium(IV) species had been formed. An explanation for the reduction of vanadium(V) to vanadium(IV) could be either the oxidation of the phenol to a quinone or the oxidative coupling of the phenol to a dimer or higher oligomer. However, neither ^{1}H NMR nor GC−MS analysis of the reaction mixtures gave any evidence for the formation of such products. Furthermore, *p*-benzoquinone is known to oxidize vanadium(IV) compounds,[19] and several vanadium(V) phenolate complexes that are stable toward reduction are known.[20] Therefore, it is unlikely that the reduction is caused by the phenolic part of the ligand. It is more likely that the amine function in the ligand is responsible for the reduction. The reduction of vanadium(V) compounds in the presence of aliphatic amines has been reported before: [$VOCl_2(NMe_3)_2$] can be synthesized by stirring [$VOCl_3$] in NMe_3.[21,22] The chloride "lost" from the vanadium(V) starting material is recovered as the ammonium salt, $HNMe_3Cl$. The more protons are present at the α-carbon atoms, the more facile the reduction becomes.[23]

Interestingly, the reduction of [$VOCl_3$] by **1** can be used as a tool for the synthesis of vanadium(IV) (bis)phenolates. By addition of at least 2.5 equiv of the phenol to [$VOCl_3$] the already known vanadium(IV) oxo (bis)phenolate [VO(O-MDMBA)$_2$] (**4**)[5] was prepared in high yield on a multigram scale (Scheme 1, ii).

To avoid reduction of the vanadium, a less electrophilic vanadium starting material was used. Vanadium arylimido (tris)diethylamides, [V(=NR)$(NEt_2)_3$] (R = Ph (**5a**), *p*-Tol (**5b**)), can be prepared via a metathesis reaction between **3a** or **3b** and 3 equiv of lithium diethylamide (Scheme 1, iii). Compounds **5a** and **5b** are obtained as dark-red oils. Attempts to prepare **5a** by refluxing **3a** in neat diethylamine were not successful. Although a reaction did take place, a mixture of unidentified products was obtained.

In order to prepare the vanadium(V) monophenolate [V(=NPh)$(NEt_2)_2$(O-MDMBA)], **5a** was reacted with 1 equiv of the parent phenol of **1**. Although quantitative conversion of **1** occurred, ^{1}H NMR analysis showed that a complicated mixture of products had formed. One of the reaction products that was isolated by selective crystallization was the vanadium(IV) species [V(=NPh)(O-MDMBA)$_2$] (**6**) (Scheme 1, iv). EPR analysis of **6** in solution at room temperature shows the expected characteristic octet structure ($A_{iso} = 85.28(1) \times 10^{-4}$ cm^{-1}, $g_{iso} = 1.9717(6)$) due to hyperfine interaction between the vanadium nucleus ($I = {}^7/_2$) and the unpaired electron. The hyperfine interactions of the nitrogens are not resolved. Recent EPR studies on vanadium(IV) oxo (bis)phenolate complexes showed that the value of the hyperfine couplings can be indicative for the electronic influence of the ligands.[5] The difference between the hyperfine couplings of **6** and **4** ($A_{iso} = 93.9 \times 10^{-4}$ cm^{-1}) is in accord with earlier observations that the phenylimido ligand is a stronger electron donor than the oxo group.[6]

In contrast to these findings, reaction of 2 equiv of **1** with either **5a** or **5b** did not result in reduction products, but instead gave the vanadium(V) (bis)phenolate complexes [V(=NR)(NEt_2)(O-MDMBA)$_2$] (R = Ph (**7a**), *p*-Tol, (**7b**)), in quantitative yields (Scheme 1, v). Unfortunately both compounds **7a** and **7b** have low thermal stability. In the solid state at −20 °C they are stable for several months at least, but at room temperature decomposition is observed within several days. In benzene solution **7b** decomposes into an unidentified paramagnetic compound within 24 h. However, the latter reduction is

(17) Spek, A. L. *Acta Crystallogr*. **1990**, *A46*, C-34.
(18) *International Tables for Crystallography*; Wilson, A. J. C., Ed.; Kluwer Academic Publishers: Dordrecht, The Netherlands, 1992; Vol C.
(19) Pasquali, M.; Landi, A.; Floriani, C. *Inorg. Chem.* **1979**, *18*, 2397.
(20) Masthoff, R.; Köhler, H.; Böhland, H.; Schmeil, F. *Z. Chem.* **1965**, *5*, 122.
(21) Baker, K. L.; Edwards, D. A.; Fowles, G. W. A.; Williams, R. G. *J. Inorg. Nucl. Chem.* **1967**, *29*, 1881.
(22) Drake, J. E.; Vekris, J.; Wood, J. S. *J. Chem. Soc. A* **1968**, 1000.
(23) Preuss, F.; Fuchslocher, E.; Leber, E.; Towae, W. *Z. Naturforsch.* **1989**, *44b*, 271.

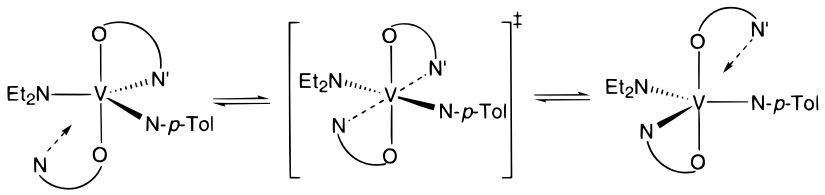

Figure 2. Fluxional behavior of compound **7b** in solution.

sufficiently slow to allow study of the structural features of **7b** in solution by NMR spectroscopy.

The ^{1}H NMR spectra of **7a** and **7b** in C_6D_6 at room temperature show one unique pattern of aminophenolate resonances. While the NMe_2 methyl groups appear as one singlet, the benzylic protons give rise to a well-resolved AB pattern, which indicates the presence of diastereotopic benzylic protons (vide infra). Both the methylene and methyl signals of the amide ligand appear as broad peaks.

To get more insight into the molecular geometry of **7b** in solution, a variable-temperature ^{1}H NMR study was carried out. The AB pattern for the benzylic protons remains the same, upon raising the temperature to 100 °C in toluene-d_8. Although the signals for the methyl and methylene protons of the diethylamide group get sharper, they remain poorly resolved. The methylene protons show up as a broad signal with some fine structure, whereas the methyl protons appear as a poorly resolved double triplet. This indicates that the methylene protons are diastereotopic as well. Lowering the temperature results in broadening of both the methyl and the methylene signals, and they decoalesce into two sets of two broad singlets at 15 and 0 °C, respectively ($\Delta G^{\ddagger} = 57$ kJ·mol^{-1}).

Further lowering of the temperature causes a broadening of the signals for the benzylic protons, and at −70 °C two poorly resolved AB patterns are observed. Apart from these changes also the signals of the NMe_2 groups and those of the methylene protons of the NEt_2 group have changed. However, the interpretation of the spectra at these low temperatures is severly hampered by extensive broadening of all peaks. In fact only the benzylic signals are separated sufficiently to give information about the possible structure of **7b**. The spectral features may be interpreted as follows.

In the slow exchange limit (below −40 °C) V−N coordination exists, which is rigid on the NMR time scale. One of the aminophenolate ligands is bonded in an η^2-O,N motif, whereas the other aminophenolate is η^1-bonded via the oxygen atom exclusively. This will result in two different AB patterns for the benzylic protons. As a consequence of the rigid η^2-O,N coordination of one of the aminophenolate ligands, one singlet for the free NMe_2 group of the η^1-O-bonded ligand and two singlets for the coordinated NMe_2 group are expected. Unfortunately this was not observed due to the extensive broadening of the signals in this region of the spectrum.

At temperatures above −40 °C the exchange between the coordinated and noncoordinated amine functionalities becomes fast on the NMR time scale and the two states, both containing one η^1-O- and one η^2-O,N-bonded aminophenolate ligand, cannot be distinguished. Therefore only one set of aminophenolate signals is observed. The prochiral benzylic protons show up as an AB pattern, since there is no molecular plane of symmetry containing the benzylic carbon atoms. The two methyl groups of the NMe_2 group appear as one singlet, because both pyramidal inversion and rotation around the benzylic carbon−nitrogen axis, which are taking place in the noncoordinated CH_2-NMe_2 groups, are processes with very small activation barriers.

On the basis of these findings we propose that **7b** is a five-coordinate species. This conclusion is corroborated by ^{51}V NMR data (vide infra). The geometry around the vanadium is best described starting from an octahedral geometry with the two aminophenolate ligands in one plane with a trans N,N-conformation. De-coordination of one of the NMe_2 groups creates a five-coordinate species with the second NMe_2 group at the top of a square pyramid. The basal plane is formed by the two oxygen atoms of the phenolate ligands and the two nitrogen atoms of the imido and amide ligand. Due to both steric hindrance and the preferred bite angle of the aminephenolate ligand of approximately 90°, this geometry distorts to a trigonal bipyramidal one with the three nitrogen atoms in the equatorial plane and the two oxygen atoms at the apical positions. This geometry was confirmed by Molecular Mechanics calculations.

The exchange between the coordinated and noncoordinated amine functionalities may happen via a facial attack of the noncoordinated amine to give a six-coordinate octahedral transition state and subsequent de-coordination of the second amine (see Figure 2). Although an inversion at the vanadium center takes place, due to the exchange between the η^1-O- and the η^2-O,N-bonded aminophenolate ligands the configuration at the vanadium center is retained as is observed by the AB pattern for the benzylic protons in the fast exchange limit. If the exchange would happen via a dissociative pathway with a four-coordinate tetrahedral transtition state, an apparent molecular plane of symmetry would be present in the fast exchange limit and the benzylic protons would show up as singlets.

At temperatures below 0 °C the two ethyl groups of the diethylamide moiety appear as two sets of broad singlets. For the two ethyl groups to be chemically unequivalent, the rotation around the V−N bond has to be slow on the NMR time scale. We attribute this slow rotation around the V−N bond to the presence of a vanadium−nitrogen double bond. A filled p-orbital is present on the nitrogen atom, and this orbital may overlap with an empty orbital on the vanadium atom and thus form a vanadium−nitrogen double bond.

Since the presence of diethylamide ligands still leaves the vanadium center too electrophilic to prevent its reduction by the amine functionality, stronger electron-donating isopropoxide ligands were used. Treatment of vanadium oxo (tris)isopropoxide (**8**) with phenyl or *p*-tolyl isocyanate in boiling octane resulted in the formation of vanadium phenyl- or *p*-tolylimido (tris)isopropoxides (**9a**,**b**) in high yields (see Scheme 2, i). Both **9a** and **9b** are stable, low-melting (53 and 43 °C) orange solids which can be crystallized from hexane. They are soluble in alkanes like pentane and hexane, in aromatics like benzene and toluene, and in polar solvents like Et_2O, CH_2Cl_2, and THF. Cryoscopic measurements in benzene showed **9b** to be monomeric in solution ($n = 1.08(2)$).

The reaction of **9b** with 1 equiv of the aminophenol **1** yielded a mixture of compounds. According to ^{1}H NMR analysis a mixture of unreacted **9b**, the vanadium(V) (mono)phenolate [V(=N-*p*-Tol)(O-MDMBA)(O-*i*-Pr)$_2$] (**10**), and the vanadium-(V) (bis)phenolate [V(=N-*p*-Tol)(O-MDMBA)$_2$(O-*i*-Pr)] (**11**)

Scheme 2

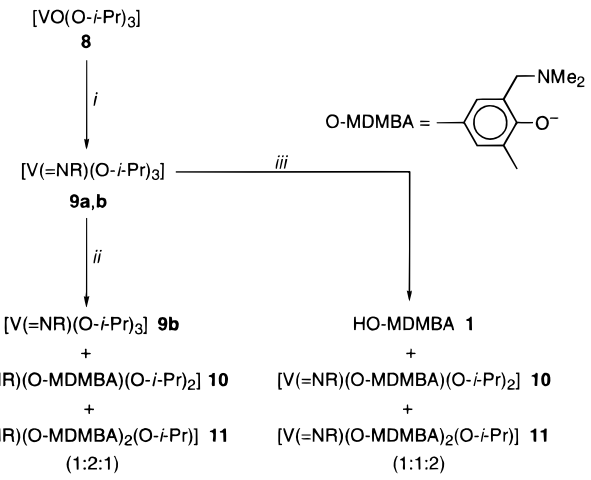

(i) R−NCO, reflux in octane (R = Ph (**a**), *p*-Tol (**b**)). (ii) R = *p*-Tol; 1 equiv of HO-MDMBA. (iii) R = *p*-Tol; 2 equiv of HO-MDMBA.

Scheme 3. Synthesis of $[VOCl_2(OCMe_2([2]\text{-Py}))]$ (**12**) and $[V(=N\text{-}p\text{-Tol})Cl_2(OCMe_2([2]\text{-Py}))]$ (**13**)

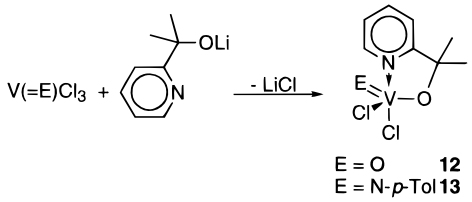

had formed (Scheme 2, ii). On the basis of the size of the signal of the methyne protons of the isopropoxy groups, the ratio of **9b**, **10**, and **11** was approximately 1:2:1.

When **9b** was reacted with 2 equiv of the aminophenol **1** again a mixture of compounds was obtained, viz., a 1:1:2 mixture of the aminophenol **1**, the (mono)phenolate **10**, and the (bis)phenolate **11** (Scheme 2, iii). This ratio is shifted upon the addition of more phenol. Reacting **9b** with 3 or 4 equiv of **1** led to the formation of mixtures of **10** and **11** in the molar ratios 1:5 and 1:9, respectively. The formation of a tris-substituted product was never observed.

Although the vanadium (mono)phenolate **10** could not be isolated as a pure compound, the characteristic signals for the isopropoxy and aminophenolate ligands were well-separated from those of the vanadium (bis)phenolate **11**. ^{1}H NMR analysis of the mixture showed two doublets for the two isopropoxy groups of **10**. The benzylic and NMe_2 signals of the phenolate ligand, however, appeared as singlets. Assuming a monomeric configuration for **10**, Molecular Mechanics calculations showed its geometry to be most likely trigonal bipyramidal. The equatorial plane would then be formed by the *p*-tolylimido unit, an isopropoxide, and the coordinating amine of the phenolate ligand. The axial positions would be occupied by the second isopropoxide and the oxygen of the phenolate ligand. However, since in such a structure two different isopropoxide groups are present, the benzylic protons would be diastereotopic and should show up as an AB pattern in the ^{1}H NMR spectrum. As this is not the case, it is unlikely that **10** is a mononuclear complex, and a dimeric structure with two bridging and two terminal isopropoxy groups similar to the solid-state structure of **9b**[9] seems to be more likely.

In order to obtain vanadium(V) complexes containing the pyridylalkoxide $[OCMe_2([2]\text{-Py})]^-$ (**2**), $[VOCl_3]$ and $[V(=N\text{-}p\text{-Tol})Cl_3]$ (**3b**) were reacted with $LiOCMe_2([2]\text{-Py})$ (see Scheme 3). In this way $[VOCl_2(OCMe_2([2]\text{-Py}))]$ (**12**) and $[V(=N\text{-}p\text{-Tol})Cl_2(OCMe_2([2]\text{-Py}))]$ (**13**) were obtained. Compound **12** is a stable orange solid which melts without decomposition at 150 °C. It is insoluble in alkanes, poorly soluble in Et_2O and aromatic solvents like benzene and toluene, but soluble in CH_2Cl_2. Compound **13** is a green solid, which is poorly soluble in most solvents. It does not melt at temperatures up to 200 °C. The ease with which these compounds are prepared and their stability toward reduction are remarkable in comparison to the partly unsuccessful attempts to prepare vanadium(V) complexes with the aminophenolate **1**. This is particularly true when it is taken into account that pyridine itself causes reduction of $[VOCl_3]$.[24] The reason for this difference is not known.

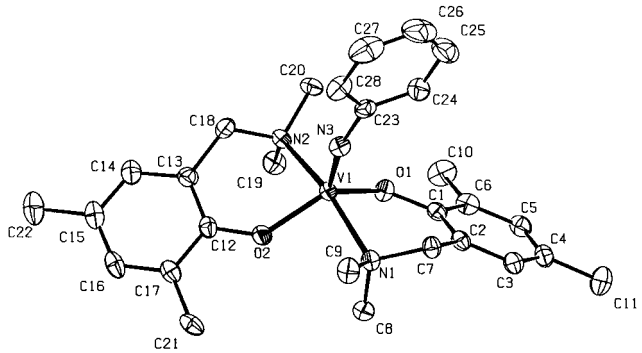

Figure 3. Displacement ellipsoid plot of **6**·Et_2O, drawn at 50% probability. Hydrogen atoms are omitted for clarity.

The ^{1}H NMR spectra of both **12** and **13** are consistent with their expected structures. The chemical shift of the hydrogen atom ortho to the pyridyl nitrogen indicates that the pyridine of the pyridylalkoxide is involved in coordination.[11,25,26] The difference between the chemical shift of the pyridine-H(6) proton in the metal complex and the parent alcohol ($\Delta\delta$) suggests that in both **12** ($\Delta\delta$ = 0.49) and **13** ($\Delta\delta$ = 0.59) the ligand is η^2-O,N-bonded to the vanadium center.

Solid-State Structures of 6 and 12. Crystallization of the vanadium imido (bis)phenolate **6** from Et_2O gave crystals suitable for X-ray diffraction analysis. Its molecular structure is depicted in Figure 3, and pertinent bond lengths and bond angles are given in Table 2. The structure of **6** is very similar to that of another vanadium(IV) (bis)phenolate compound, $[VO(OC_6H_4(CH_2NMe_2)\text{-}2)_2]$.[5] The vanadium is surrounded in a trigonal bipyramidal fashion with a considerable distortion toward a square pyramidal geometry (39% on the Berry pseudorotation path between D_{3h} and C_{4v} [27] vs 37% for the oxo compound). The oxygen atoms of the aminophenolate ligand (O1 and O2) and the nitrogen atom of the imido group (N3) form the equatorial plane. The amino nitrogen atoms (N1 and N2) occupy the apical positions. The V−O, V−N, and O−C distances as well as the bite angles of the phenolate ligands (O−V−N) are comparable with those in the oxo compound $[VO(OC_6H_4(CH_2NMe_2)\text{-}2)_2]$, whereas the N1−V1−N2 angle is slightly smaller (163.72(10)° vs 165.13(11)° in the oxo compound).

A second pseudopolymorph of compound **6** has been found after crystallization from benzene at room temperature. Although both crystal structures are triclinic with a *P*$\bar{1}$ space group and

(24) Funk, H.; Weiss, W.; Zeising, M. *Z. Anorg. Chem.* **1958**, *296*, 36.
(25) van der Schaaf, P. A.; Abbenhuis, R. A. T. M.; van der Noort, W. P. A.; de Graaf, R.; Grove, D. M.; Smeets, W. J. J.; Spek, A. L.; van Koten, G. *Organometallics* **1994**, *13*, 1433.
(26) Brandts, J. A. M.; Boersma, J.; Spek, A. L.; van Koten, G. *Eur. J. Inorg. Chem.* **1999**, 1727.
(27) Holmes, R. R. *Prog. Inorg. Chem.* **1984**, *32*, 119 and references therein.

Table 2. Selected Bond Lengths and Bond Angles for **6**·Et_2O, **6**·C_6H_6, and **12**

	6·Et_{2O}	**6**·C_{6H6}	**12**
	Bond Lengths (Å)		
V1−O1	1.887(2)	1.901(2)	1.578(3)
V1−O2	1.911(2)	1.911(2)	1.763(3)
V1−N1	2.164(2)	2.167(3)	2.163(3)
V1−N2	2.168(2)	2.181(3)	
O1−C1	1.351(5)	1.348(4)	
O2−C12	1.340(4)	1.349(4)	
V1−Cl1			2.2282(14)
V1−Cl2			2.2195(14)
V1−N3	1.685(3)	1.681(3)	
N3−C23	1.370(5)	1.376(4)	
O2−C1			1.435(4)
	Bond Angles (deg)		
O1−V1−N1	87.69(10)	87.90(11)	89.48(14)
O2−V1−N2	87.16(10)	87.72(11)	
V1−N3−C23	161.7(2)	174.2(3)	
V1−O1−C1	133.6(2)	133.0(2)	
V1−O2−C12	134.1(2)	133.7(2)	
O1−V1−O2	129.83(12)	125.37(11)	113.17(13)
O2−V1−N3	117.14(12)	118.88(12)	
O1−V1−N3	113.03(12)	115.73(12)	
N1−V1−N2	163.72(10)	168.38(11)	
O1−V1−Cl2			110.64(10)
O2−V1−Cl2			131.29(9)
O1−V1−Cl1			103.57(10)
N1−V1−Cl1			166.31(10)
N1−V1−O2			75.39(12)
N1−V1−Cl2			84.85(11)
V1−O2−C1			129.8(2)

the unit cells have approximately the same size, the unit cell dimensions are different. Also the molecular structure of **6**·C_6H_6 is different. The geometry around the vanadium center is less distorted toward a square pyramid (24% on the Berry pseudorotation path), which is visible in the slightly larger N1−V−N2 angle of 168.38(11)°. More remarkable is the much larger V−N3−C23 angle of 174.2(3)° vs 161.7(2)°. Both polymorphs contain 1 equiv of the solvent from which they were crystallized, and the steric interference exerted by these solvent molecules causes the observed geometrical differences. In the polymorph obtained from benzene the solvent molecule is located opposite to the imido functionality at the O1−N1−O2−N2 face. This position can be considered as the sixth coordination side, and steric interference from the benzene molecule on the imido functionality is expected to be negligible. In the polymorph obtained from Et_2O, however, the Et_2O molecule is located next to the imido functionality at the O1−N1−N3 face. In this way it forces the imido functionality to bend away from its ideal position, and as a result a smaller V−N3−C23 angle is found. A smaller V−N−C angle could point to a decreased V−N bond order. However, this is not reflected by a longer V−N bond length in the molecular structure of **6**·Et_2O. From these observations it can be concluded that bond angles around vanadium, as derived from molecular geometries of vanadium complexes in the solid state, should be handled with care.

Crystals of **12** suitable for an X-ray structure determination were obtained from a 1:1 mixture of CH_2Cl_2 and Et_2O at −20 °C. The molecular structure is depicted in Figure 4 (see Table 2 for relevant bond lengths and angles). The geometry around the vanadium center is a very distorted trigonal bipyramid (41% on the Berry pseudorotation path). The equatorial plane is formed by the two oxygen atoms O1 and O2 and by one of the chlorine atoms, Cl2. The axial positions are occupied by the pyridyl nitrogen atom N1 and the second chlorine atom Cl1. The V−O distance (1.763(3) Å) falls in the range reported for

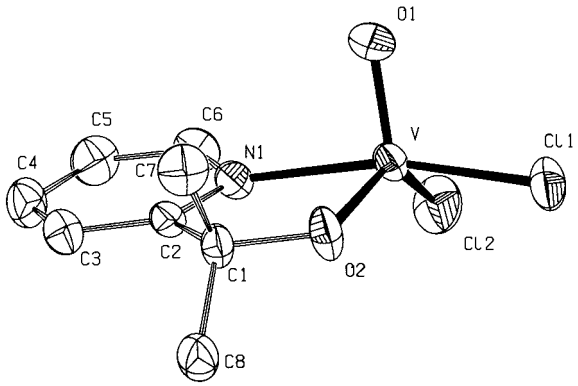

Figure 4. Displacement ellipsoid plot of **12**, drawn at 50% probability. Hydrogen atoms are omitted for clarity.

other vanadium(V) alkoxo compounds (1.74−1.99 Å).[28−30] However, the V−Cl and the V═O distances (av 2.23 and 1.578(3) Å, respectively) are among the shortest ever reported. Also in view of the small bite angle of the η^2-O,N-chelate bonded pyridylalkoxide ligand of 75.39(12)°, this structure is probably best described starting from a tetrahedral geometry. The vanadium center is surrounded by two oxygen and two chlorine atoms. Facial attack of the pyridyl nitrogen at the O1−Cl2−O2 face creates a pseudo-five-coordinate structure following an S_N2 type of reaction coordinate. This view seems corroborated by the fact that the V−Cl1 distance is slightly lengthened.

^{51}V NMR Spectroscopy. The ^{51}V nucleus is well suited for NMR studies because of its high abundance (99.76%) and high sensitivity (0.382 relative to that of the ^{1}H nucleus at equal field strength). The vanadium NMR data of the arylimido compounds and those of related oxo vanadium(V) compounds are listed in Table 3. The chemical shifts range from $\delta = 305$ ppm for [V(═N-*p*-Tol)Cl_3] to $\delta = -624$ ppm for [VO(O-*i*-Pr)$_3$]. For compounds **5a**,**b** and **9a**,**b** the signals are split up in a 1:1:1 triplet (partly resolved for **5a**,**b**) with coupling constants of approximately 100 Hz due to the coupling with the ^{14}N atom ($I = 1$) of the imido functionality. The chemical shifts of the arylimido compounds follow the so-called "inverse halogen dependence" in which the nucleus becomes more shielded with increasing electronegativity of the substituents: δ [V(═NR)Cl_3] > δ [V(═NR)$(NEt_2)_3$] > δ [V(═NR)(O-*i*-Pr)$_3$].

This inverse halogen dependence is also visible for the arylimido functionality itself. Even though it is a stronger electron donor than the oxo group (vide supra), due to the less electronegative nitrogen atom it has a deshielding influence on the vanadium nucleus as compared to the oxo functionality. However, this effect weakens with the introduction of increasingly more electronegative, π-donating ligands, something which has also been observed in the series [V(═N-*p*-Tol)Cl_{3-x}(O-*t*-Bu)$_x$] ($x = 0-3$) in comparison with the analogous oxo compounds.[7]

The ^{51}V chemical shifts do not provide information about the coordination number since the increase in the sum of electronegativities of bonded atoms is counteracted by the expansion of the coordination sphere.[12] However, Crans and Shin showed that a relation between the inverse line width and the chemical shift might exist.[31] Two distinct clusters were found

(28) Caughlan, C. N.; Smith, H. M.; Watenpaugh, K. *Inorg. Chem.* **1966**, *5*, 2131.
(29) Glas, H.; Herdtweck, E.; Artus, G. R. J.; Thiel, W. R. *Inorg. Chem.* **1998**, *37*, 3644.
(30) Crans, D. C.; Keramidas, A. D.; Amin, S. S.; Anderson, O. P.; Miller, S. M. *J. Chem. Soc., Dalton Trans.* **1997**, 2799.
(31) Crans, D. C.; Shin, P. K. *J. Am. Chem. Soc.* **1994**, *116*, 1305.

Table 3. ^{51}V NMR Data of Various Vanadium(V) Compounds[a]

compound	δ (ppm)	$\Delta\nu_{1/2}$ (Hz)	$^1J_{^{51}V,^{14}N}$ (Hz)	ref
[V(=NPh)Cl_3] (**3a**)	252	530		this work
[V(=N-*p*-Tol)Cl_3] (**3b**)	305	500		7
[VO(NEt_2)$_3$]	−389			32
[V(=NPh)(NEt_2)$_3$] (**5a**)[c]	−172	276	97[b]	this work
[V(=N-*p*-Tol)(NEt_2)$_3$] (**5b**)[c]	−175	275	99[b]	this work
[VO(O-*i*-Pr)$_3$] (**8**)	−624	13		this work
[V(=NPh)(O-*i*-Pr)$_3$] (**9a**)	−622		113	this work
[V(=N-*p*-Tol)(O-*i*-Pr)$_3$] (**9b**)	−611		114	this work
[V(=N-*p*-Tol)(NEt_2)(O−MDMBA)$_2$] (**7b**)[c]	−253	137		this work
[V(=N-*p*-Tol)(O-MDMBA)(O-*i*-Pr)$_2$] (**10**)	−444	450		this work
[V(=N-*p*-Tol)(O-MDMBA)$_2$(O-*i*-Pr)] (**11**)	−358	808		this work
[$VOCl_2$(O-*i*-Pr)] (**14**)	−309			32
[$VOCl_2$(OCMe$_2$([2]-Py))] (**12**)	−235	93		this work
[V(=N-*p*-Tol)Cl_2(OCMe$_2$([2]-Py))] (**13**)	33	1100		this work

[a] $CDCl_3$, 78.9 MHz, relative to external [$VOCl_3$]/$CDCl_3$ (75/25 v/v). [b] Partially resolved triplet. [c] In C_6D_6.

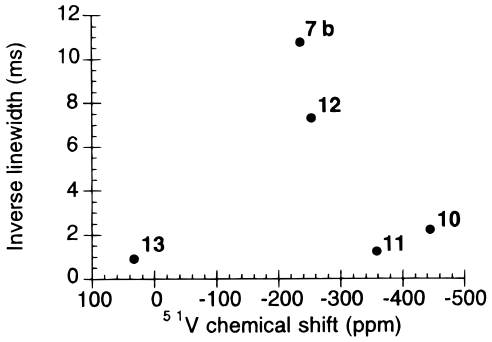

Figure 5. Inverse line width, $\Delta\nu_{1/2}{}^{-1}$, plotted as a function of the ^{51}V NMR chemical shifts for vanadium(V) complexes.

when the inverse line width was plotted against the chemical shift of a series of vanadium(V) complexes. For five-coordinate complexes a cluster was found in the quadrant defined by the inverse line width values of 5−8 and chemical shift range −480 to −490 ppm. The second cluster containing six-coordinate complexes occupied the area with inverse line width values of 1−4 and chemical shift range −490 to −526 ppm. The value of 4 for the inverse line width appears to be the approximate border value between five- and six-coordinate vanadium species. The chemical shifts found for the complexes reported here do not fall into these ranges, but since Crans and Shin examined only *cis*-dioxo vanadium(V), complexes this is not surprising. What is more important is that they found that coordination of a second amine function does not significantly change the chemical shift but only affects the value of the inverse line width. In a plot of the inverse line width against the chemical shift of the vanadium(V) complexes containing O,N-chelating ligands (see Figure 5), two areas can be recognized: viz., one with an inverse line width value smaller than 4 containing compounds **10**, **11**, and **13** and one with values larger than 4 containing compounds **7b** and **12**. According to the X-ray structure, **12** is a five-coordinate species. We therefore tentatively propose **7b** to be five-coordinate as well, which was already concluded from its dynamic behavior in the ^{1}H NMR (vide supra). For compounds **10**, **11**, and **13** a six-coordinate structure is expected. On the basis of its ^{1}H NMR data, a dimeric structure with two bridging and two terminal isopropoxy groups was proposed for **10**. This implies that the amine function must be coordinated to make it a six-coordinate species. For compound **13** to be six-coordinate it has to be dimeric as well. Whether the dimer is bridged via chlorine atoms or imido functionalities remains inconclusive from these data.

Polymerization Tests. The compounds **12** and **13** were tested in ethene polymerization together with several other nonchelated vanadium(V) oxo and imido compounds. Whereas **12** displayed a reasonable activity (88 kg PE/mol[V]·h·bar at 50 °C), **13** showed almost no activity under similar circumstances and for both complexes the activities were much lower than those of the nonchelated counterparts. We tentatively assign this decrease in activity to a lower number of catalytically active species (for more details see the Supporting Information).

Acknowledgment. This work was carried out in connection with NIOK, The Netherlands Institute for Catalysis Research, and was supported by the Department of Economic Affairs of The Netherlands. Polymerization tests and polymer analysis were carried out at the Center for Catalytic Olefin Polymerization in Groningen, The Netherlands. Thanks are due to E. A. C. Brussee and A. Jekel for technical assistance. Crystallographical studies were supported in part (A.L.S., M.L.) by the Councel for the Chemical Sciences of the Netherlands Organization for Scientific Research (CW-NWO). EPR analyses were carried out at the Department of Atomic and Interface Physics, Utrecht University, The Netherlands, by Dr. E. E. van Faassen.

Supporting Information Available: Detailed information on polymerization activity and X-ray crystallographic files in CIF format for the structures of **6**·Et_2O, **6**·C_6H_6, and **12**. This material is available free of charge via the Internet at http://pubs.acs.org.

(32) Priebsch, W.; Rehder, D. *Inorg. Chem.* **1985**, *24*, 3058.

IC991415S